Restructuring of Cobalt Nanoparticles Induced by Formation and Diffusion of Monodisperse Metal-Sulfur Complexes

J. Kibsgaard,[1] K. Morgenstern,[2] E. Lægsgaard,[1] J. V. Lauritsen,[1] and F. Besenbacher[1,*]

[1]*Interdisciplinary Nanoscience Center (iNANO) and Department of Physics and Astronomy, University of Aarhus, DK-8000 Aarhus C, Denmark*

[2]*Institut für Festkörperphysik, Leibniz Universität Hannover, Appelstr. 2, D-30167 Hannover, Germany*

(Received 13 November 2007; published 21 March 2008)

Time-resolved scanning tunneling microscopy (STM) is used to investigate a massive sulfur-induced transformation of a homogeneous array of ~2 nm Co nanoparticles into a new cobalt sulfide phase. The underlying atomistic mass-transport process is revealed and, surprisingly, found to be mediated exclusively by the formation and detachment of monosized Co_3S_4 complexes at the perimeter of the Co nanoparticles. The process is followed by fast diffusion, agglomeration of the complexes, and subsequent crystallization into a cobalt sulfide phase.

DOI: 10.1103/PhysRevLett.100.116104 PACS numbers: 68.35.Fx, 68.37.Ef, 68.43.Jk

When surfaces are exposed to a gaseous environment, a massive shift in the surface morphology may be initiated by the interaction with gas molecules [1]. The process of adsorbate-induced diffusion is in general very central to, e.g., thin film growth, etching, corrosion, growth of nanostructures, and sintering in heterogeneous catalysis [2,3]. However, the details of the underlying physical processes such as adsorption, diffusion, and nucleation are often far from understood. Much knowledge has been gained by studies on single crystal surfaces, but key issues related to the atomistic nature of the species mediating the mass-transport often remain unsolved. Detailed insight into such processes for complex systems consisting of nanoparticles with multiple facets has, furthermore, been extremely difficult to achieve due to lack of techniques with the appropriate spatial and temporal resolution. Scanning tunneling microscopy (STM) is the technique of choice for revealing the atomic-scale realm of matter. More specifically STM offers the possibility to directly observe dynamics of adsorbate-induced transformations even on nanoparticles and furthermore it is possible directly to identify diffusing species in time-resolved STM movies [4]. For example, STM was used to show that the diffusivity of a Pt-H complex is greatly enhanced relative to single Pt adatoms on the Pt(110) surface [5]. In another recent study, STM was used to show that the dynamics of Cu-ripening on a Cu surface were enhanced by several orders of magnitude in the presence of trace amounts of sulfur [6]. Interestingly, the enhanced mass transport was found not to be related to the formation of a simple diatomic complex (e.g., Cu-S) as in the former example, but from an interplay with theoretical density functional theory (DFT) studies [7] the results were explained by the formation and enhanced diffusion of particularly stable Cu_3S_3 clusters, which formed only at the island edges.

In this Letter, we present high-resolution, time-resolved dynamic STM studies of Co nanoparticles supported on a Au(111) surface in order to investigate the detailed atomic mechanisms involved in adsorbate-induced transformations for a nanoparticle system exposing multiple facets. In-situ STM movies recorded in a mild sulfiding environment over an extended time scale of up to 80 hours show that very significant restructuring and agglomeration of the Co nanoparticles occur at room temperature. During continuous sulfur exposure, a significant mass transport of Co is revealed, and the restructuring process continues until all metallic Co has been converted into a larger homogeneous cobalt sulfide phase. The findings contrast the general expectation from single crystal studies [8] that the main effect of sulfur is to cover the metallic surface by a sulfide. Our analysis of high-resolution STM movies directly reveals the atomic mechanisms involved, and we show that the atomic-scale mass transport is mediated by a volatile monosized Co_3S_4 nanocluster that continuously forms at the perimeter of the Co nanoparticles and diffuses rapidly and agglomerates into a cobalt sulfide phase.

The sulfur-induced process was monitored *in situ* with the fast-scanning Aarhus STM [9] housed in a UHV chamber. Co nanoparticles were grown by deposition of Co (0.28 ML) onto a sputter-cleaned Au(111) substrate exposing the well-known herringbone reconstruction, which acts as a template for Co nanoparticles with a uniform size and shape [10–12] [see Fig. 1(a)]. Co nanoparticles synthesized under these conditions were previously observed at RT to be static on the Au(111) surface and were characterized as truncated triangular, bilayer particles oriented with the close-packed Co(0001) [or Co(111)] facet in parallel with the substrate [12]. Less than 5% of the nanoparticles had Co also in the third layer.

In Fig. 1 is depicted snapshots from the STM movie M1 [13] recorded over a time span of 80 h while exposing the crystal to $\sim 5 \times 10^{-8}$ mbar H_2S. The STM movie reveals a massive redistribution of the Co nanoparticles induced by the introduction of H_2S. From the individual frames of the

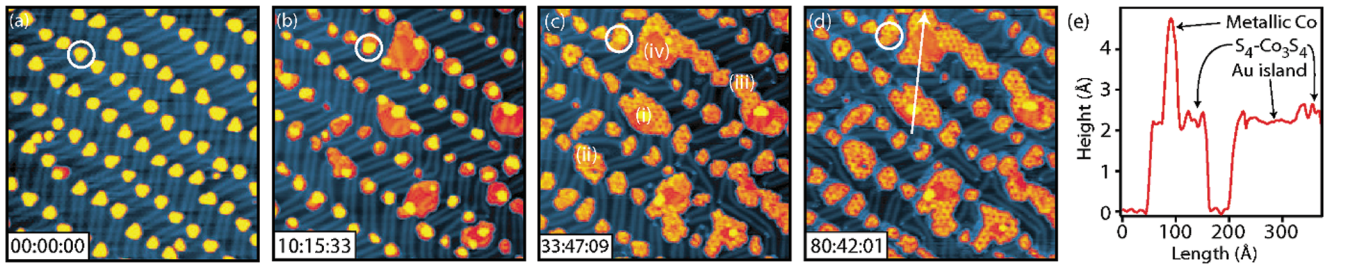

FIG. 1 (color). (a)–(d) Time lapse sequence of STM images (700 Å × 700 Å, $I_t = 0.6$ nA, $V_t = -1.25$ V) from a STM movie of ~80 h(movie M1 in Ref. [13]). Co particles exposed to H_2S are gradually transformed into cobalt sulfide. A reference particle has been encircled. Four different phases are observed: (i) The metallic Co phase, (ii) Amorphous cobalt sulfide, (iii) Crystalline cobalt sulfide, and (iv) Au islands. Time in (h:min:s). (e) Line scan [position indicated by arrow in (d)] showing the height of the different phases.

STM movie [see example in Fig. 1(c)] we can directly identify three involved primary phases by their atomic-scale structure and apparent height from STM line scans; (i) metallic Co nanoparticles, (ii) amorphous cobalt sulfide, and (iii) crystalline cobalt sulfide [14].

The steps of the decay of the Co nanoparticles and the corresponding growth of cobalt sulfide are illustrated in Fig. 2(a), where the areas have been measured directly in the STM images extracted from movie M1. In this analysis, we do not discriminate between crystalline and amorphous cobalt sulfide. As seen from Fig. 2(a) the decay rate of the Co nanoparticles (circles and red curve) is initially very fast, but after a duration of ~80 min, the decay rate decreases quite abruptly. Similar abrupt changes in the decay rate are also observed after ~1000 and ~1500 min. The formation rate of the cobalt sulfide phase (triangles and blue curve) is seen to correlate exactly with the features of the Co nanoparticle decay.

Several different decay scenarios are possible for the cobalt nanoparticles, since it may correlate with (i) the particle area ($dA/dt \propto A$), (ii) the particle perimeter (circumference) ($dA/dt \propto \sqrt{A}$), or (iii) simply the arrival rate of sulfur ($dA/dt = \text{const}$). We find that option number (ii) is preferred, since a $\sqrt{A} \propto -t$ correlation is found both in analysis of large-scale images Fig. 2(a) and in another more precise analysis of a single bilayer Co nanoparticle imaged with a higher time resolution [Fig. 2(b)]. From the decay curves, we therefore conclude that the sulfur-induced corrosion process depends on the number of available sites on the perimeter of the nanoparticles. We thus propose a model in which the H_2S is initially physisorbed on the Au surface [15] (and not exclusively on the Co nanoparticles) and then diffuses to the cobalt nanoparticles and extracts the Co from perimeter sites. In the STM image in Fig. 3(c) recorded at 163 K the physisorbed H_2S can be seen directly as a striped phase.

To identify the diffusing species responsible for the mass transport we have recorded a movie with even higher time resolution. The movie M2 [13] shows two Co nanoparticles exposed to H_2S and it clearly illustrates how largish features disappear or reappear near the perimeter between consecutive frames in the STM movie [see inset in Fig. 3(a)]. These results indicate that the decay process is

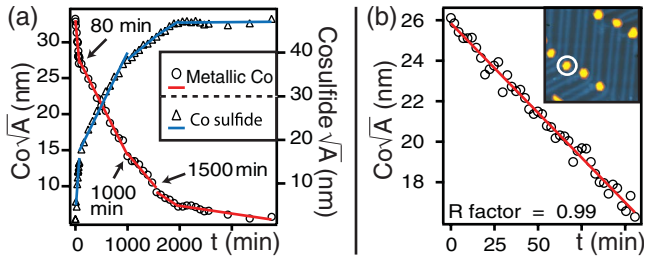

FIG. 2 (color). (a) Time evolution of cobalt nanoparticles and the cobalt sulfide, plotted as the square root of the area (from movie M1). (b) Same plot but from a second movie with higher resolution (see inset).

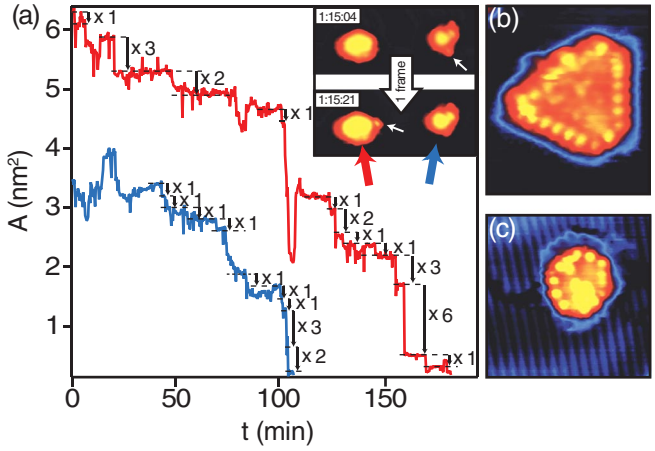

FIG. 3 (color). (a) Time evolution of the two cobalt nanoparticles (from movie M2 [13]). The movie and plot shows how monosized complexes disappear and appear between consecutive scans. (b) STM image (68 Å × 80 Å, $I_t = 0.5$ nA, $V_t = -1.25$ V) of a Co particle exposed to H_2S and subsequently imaged at 173 K. (c) STM image (40 Å × 40 Å, $I_t = 0.53$ nA, $V_t = -625$ mV, $T = 163$ K) of a Co particle surrounded by a striped structure attributed to physisorbed H_2S.

mediated by a complex larger than that of a single Co and S atom. The temporal evolution of the two nanoparticles [Fig. 3(a)] shows that the decay of the particle area, which from the curve in Fig. 2 seemed to be continuous, actually consists of steps corresponding closely to complexes of a given size. The steps are, as indicated in Fig. 3(a), all integral multiples of a smallest step size which is found to be 20 ± 2 Å^2, suggesting that the decay proceeds stepwise by the formation of single monosized type of mobile Co_nS_m complex. We could image this Co_nS_m complex in more detail by performing a quench-and-look STM experiment. The sample was exposed to H_2S at room temperature and after a few minutes transferred into the cooled STM. In the resulting STM image in Fig. 3(b) recorded at 173 K, the perimeter of the nanoparticle contains several round protrusions with a size of 21 ± 2 Å^2, which is in full accordance with the complex size in Fig. 3(a).

The formation of a rim of amorphous cobalt sulfide complexes may explain the decrease in the decay rate of the Co nanoparticles which is observed around 80 min in the graph of Fig. 2(a). The reduced decay rate can be explained by the gradual saturation of sites at the rim, which hinders the sulfur from directly accessing the remaining metallic Co. The changes in the slope of the graph in Fig. 2(a) observed at later times corresponding to ~1000 min and ~1500 min are due to the fact that the rather few three-layer-high Co nanoparticles present in the movie M1 have a much slower apparent decay rate than the two-layer high nanoparticles. The higher stability of the three-layer-high particles in the sulfiding atmosphere again suggests that H_2S mainly interacts at the interface between the Au substrate and the perimeter of the Co nanoparticles.

The cobalt sulfide phase is initially amorphous, but eventually all Co crystallizes into a structure which appears with a characteristic "mill-wheel" feature [Figs. 1(a)–1(d)]. The cobalt sulfide has an apparent height of 2.60 Å, and its top facet consists of hexagonally arranged protrusions with a lattice distance of 3.4 ± 0.1 Å [inset Fig. 4(a)]. Cobalt sulfides exist in a variety of different crystallographic structures with the Co:S ratio ranging from 9:8 in Co_9S_8 (pentlandite) to 1:2 in CoS_2 (cattierite) [16]. The observed interatomic distances in the "mill-wheel" structure matches, however, only those of the S atoms in Co_3S_4 ($d = 3.37$ Å). In support of this assignment, a recent XRD study showed that the most stable phase is indeed Co_3S_4 [17] when sulfur is in large excess. Furthermore, in a geometrical structure simulation [Fig. 4(c)] we also find excellent accordance with the mill-wheel structure observed experimentally in Fig. 4(a). The simulations were performed computationally by allowing the atoms in each layer of a single cobalt sulfide overlayer to make a vertical relaxation dependent on the position of atoms in the layer beneath and subsequently coloring of the topmost sulfur atoms in a ball model of the slabs according to the vertical relaxation. The fixed rotation of the overlayer could be determined in atom-resolved images (not shown). The resulting simulation of Co_3S_4 shows a clear hexagonal structure consisting of triangles similar in size to those observed in Fig. 4(a). Furthermore, the three corner S atoms where the triangles join have a low vertical position as indicated by the dark color, which is also in agreement with the experimentally observed STM images. The rather intriguing mill-wheel structure is therefore explained by a simple Moiré structure reflecting the lattice mismatch between the nonrotated overlayer and substrate [18].

A detailed ball model of the Co_3S_4 structure is shown in Fig. 4(b). The structure can be viewed as a network structure composed of Co_3S_4 subunits held together by an additional four sulfur ligands. The expected size and shape of this subunit matches closely the 20–21 Å^2 in size diffusing complexes observed in the low-temperature STM image [Fig. 3(b)] and quantized step decay of Co particles in Fig. 3(a). The expected height of the resulting S-Co-S layered configuration is from the bulk Co_3S_4 structure found to be 2.57 Å in good agreement with the STM observations. Because of the stacking sequence Au(111)-S_4-Co_3S_4, the overall stoichiometry corresponds

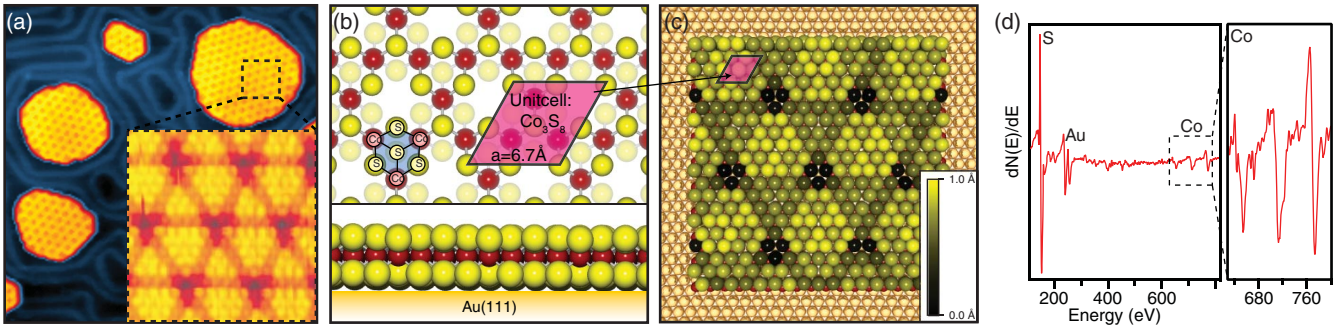

FIG. 4 (color). (a) STM image (700 Å × 700 Å) showing cobalt sulfide islands after annealing to 523 K for 30 min. Inset: An atom-resolved STM image (50 Å × 50 Å, $I_t = 0.26$ nA, $V_t = -19.5$ mV) of the cobalt sulfide. (b) Ball model, top and side view, respectively, of Au(111)-S_4-Co_3S_4. (c) Ball model of the S_4-Co_3S_4 structure on Au(111) where the color of the topmost layer of sulfur atoms represent the vertical positions. (d) AES spectrum of the S_4-Co_3S_4 structure.

to a sulfur to cobalt ratio of 8 to 3, which is higher than that observed for any bulk cobalt sulfide phase. Auger electron spectroscopy (AES), however, confirms this structure. For this analysis we synthesized larger more homogenous patches of the S_4-Co_3S_4 mill-wheel structure by annealing the sample at 523 K in a H_2S atmosphere as shown in Fig. 4(a). A control AES spectrum under the same sulfidation conditions but without Co showed no traces of sulfur, confirming that all sulfur is indeed present as cobalt sulfide. Taking Auger selectivity factors into account the peak-to-peak intensity of the AES spectrum [Fig. 4(d)] yields a sulfur to cobalt ratio of 2.7 ± 0.2 in perfect accordance with a 8 to 3 S:Co ratio. The stabilization of the sulfur excess is not surprising since the Au surface generally has a high affinity towards single-bonded sulfur compounds, such as thiols [19].

An important conclusion from the present studies is that Co nanoparticles are structurally unstable in an even very mildly sulfiding environment. STM movies with a duration of up to 80 hours directly reveal that Co nanoparticles decay by a mechanism which involves the formation of volatile Co_3S_4 complexes at the cluster perimeter. The complexes are continuously transported away, and the process should therefore occur for Co particles of any larger size also. Interestingly, the whole process occurs with a very low energy barrier since it is observed at room temperature, and the implications are that sulfur levels, even at a fraction of a ppb, will significantly influence the distribution of Co. The present findings are thus of general interest for controlling the long-term stability of systems relying on a high dispersion of Co nanoparticles such as the Co-based Fischer-Tropsch catalyst [3] and show that modeling the dynamical behavior of such systems in a sulfiding environment need to take Co_3S_4 complexes into account. Our findings suggest that the well-known catalytic deactivation mechanism by sulfur poisoning may not only be due to site-blocking by sulfur, but also be determined by an accelerated redistribution and sintering or even refacetting of the active Co nanoparticles, which may prevent full regeneration after exposure to sulfur.

Haldor Topsøe A/S is gratefully acknowledged for financial support. J. V. L. furthermore acknowledges financial support from the Carlsberg Foundation.

*fbe@inano.dk

[1] D. J. Coulman, J. Wintterlin, R. J. Behm, and G. Ertl, Phys. Rev. Lett. **64**, 1761 (1990); J. D. Batteas, J. C. Dunphy, G. A. Somorjai, and M. Salmeron, Phys. Rev. Lett. **77**, 534 (1996); E. K. Vestergaard, R. T. Vang, J. Knudsen, T. M. Pedersen, T. An, E. Lægsgaard, I. Stensgaard, B. Hammer, and F. Besenbacher, Phys. Rev. Lett. **95**, 126101 (2005).

[2] K. A. Fichthorn and M. Scheffler, Phys. Rev. Lett. **84**, 5371 (2000); J. de la Figuera, C. B. Carter, N. C. Bartelt, and R. Q. Hwang, Surf. Sci. **531**, 29 (2003); P. L. Hansen, J. B. Wagner, S. Helveg, J. R. Rostrup-Nielsen, B. S. Clausen, and H. Topsøe, Science **295**, 2053 (2002).

[3] G. L. Bezemer, J. H. Bitter, H. P. C. E. Kuipers, H. Oosterbeek, J. E. Holewijn, X. Xu, F. Kapteijn, A. J. van Dillen, and K. P. de Jong, J. Am. Chem. Soc. **128**, 3956 (2006).

[4] T. R. Linderoth, S. Horch, E. Lægsgaard, I. Stensgaard, and F. Besenbacher, Phys. Rev. Lett. **78**, 4978 (1997).

[5] S. Horch, H. T. Lorensen, S. Helveg, E. Lægsgaard, I. Stensgaard, J. K. Nørskov, K. W. Jacobsen, and F. Besenbacher, Nature (London) **398**, 134 (1999).

[6] W. L. Ling, N. C. Bartelt, K. Pohl, J. de la Figuera, R. Q. Hwang, and K. F. McCarty, Phys. Rev. Lett. **93**, 166101 (2004).

[7] P. J. Feibelman, Phys. Rev. Lett. **85**, 606 (2000).

[8] M. Foss, R. Feidenhansl, M. Nielsen, E. Findeisen, T. Buslaps, R. L. Johnson, F. Besenbacher, and I. Stensgaard, Surf. Sci. **296**, 283 (1993); J. A. Rodriguez and J. Hrbek, Acc. Chem. Res. **32**, 719 (1999).

[9] E. Lægsgaard, F. Besenbacher, K. Mortensen, and I. Stensgaard, J. Microsc. **152**, 663 (1988).

[10] J. V. Barth, H. Brune, G. Ertl, and R. J. Behm, Phys. Rev. B **42**, 9307 (1990).

[11] B. Voigtländer, G. Meyer, and N. M. Amer, Phys. Rev. B **44**, 10 354 (1991).

[12] K. Morgenstern, J. Kibsgaard, J. V. Lauritsen, E. Lægsgaard, and F. Besenbacher, Surf. Sci. **601**, 1967 (2007).

[13] See EPAPS Document No. E-PRLTAO-100-027811 for the STM movies M1 and M2. M1 directly shows the transformation of Co nanoparticles into large patches consisting of cobalt-sulfide when exposed to H_2S. M2 shows how monosized complexes disappear and appear between consecutive scans. For more information on EPAPS, see http://www.aip.org/pubservs/epaps.html.

[14] Note that a fourth structure (iv), which we identified in atom-resolved STM images (not shown) as single-layer gold islands, is present.

[15] A. J. Leavitt and T. P. Beebe, Jr., Surf. Sci. **314**, 23 (1994).

[16] S. Geller, Acta Crystallogr. **15**, 1195 (1962); D. Lundqvist and A. Westgren, Z. Anorg. Allg. Chem. **239**, 85 (1938); N. Elliott, J. Chem. Phys. **33**, 903 (1960).

[17] Y. Yin, R. M. Rioux, C. K. Erdonmez, S. Hughes, G. A. Somorjai, and A. P. Alivisatos, Science **304**, 711 (2004).

[18] F. Grey and J. Bohr, Europhys. Lett. **18**, 717 (1992).

[19] G. Poirier, Chem. Rev. **97**, 1117 (1997).